DOI: 10.1002/chem.200600076

"Pocket Dendrimers" as Nanoscale Receptors for Bimolecular Guest Accommodation

Satoshi Shinoda, Masakazu Ohashi, and Hiroshi Tsukube*[a]

Abstract: A new series of dendrimer receptors was prepared by combining a (tetraphenylporphinato)zinc(II) core and benzyl ether type dendritic substituents. Since one direction of the (tetraphenylporphinato)zinc(II) was not substituted by a dendritic residue, the resulting unsymmetrical dendrimers have "pockets" available for access of external substrates. Molecular modeling, NMR measurements, and zinc-coordination experiments revealed that the third-generation dendrimer of this type exhibited characteristic inclusion of coordinative pyridine guests. When diamidopyridine moiety was introduced into the dendrimer pocket, a thymine derivative was bound through complementary hydrogen bonding. Two different kinds of substrates, pyridine and thymine derivatives, were simultaneously accommodated in the nanoscale pocket and bimolecular guest accommodation was realized with the designed dendrimer receptor.

Keywords: dendrimers · host–guest systems · hydrogen bonds · NMR spectroscopy · supramolecular chemistry

Introduction

Bimolecular guest accommodation is one of the most important phenomena in enzymatic reactions and other biological recognition processes. When two different kinds of reactive guests are typically bound at the enzyme active center, the proximity and orientation remarkably increase reaction efficiency and selectivity. Several types of cage-like receptors have been designed to mimic such bimolecular guest accommodation.[1] Rebek and co-workers demonstrated that various molecular capsules promoted a Diels–Alder reaction based on co-encapsulation of the reactive partners.[1] Raymond et al. and Fujita et al. developed nanoscale molecular vessels composed of metal complexes that had enough large cavities to accommodate two or more guest species.[1] A series of metalloporphyrin dendrimers is a promising alternative, because they have more flexible and open structures with wide variations of porphyrin cores, branches, terminals, and other functionalized substituents.[2,3] Aida et al. and Suslick et al. reported pioneering works on molecular recognition with zinc–porphyrin dendrimers in which external coordinative guests interpenetrated into the dendrimer spheres to form the zinc-coordination complexes.[4] In addition to the regularly branched, spherical dendrimers, several unsymmetrical dendrimers have protein-like nonspherical structures.[5,6] Percec et al. reported self-assembled dendrimers from AB_3- and AB_2-type dendritic blocks.[5] Kaifer et al. introduced redox-active viologen units located at the apical positions of dendrimers.[6] We also developed unsymmetrical "proteo-dendrimers" for the complementary recognition of cytochrome *c* proteins.[7] Although several types of dendrim-

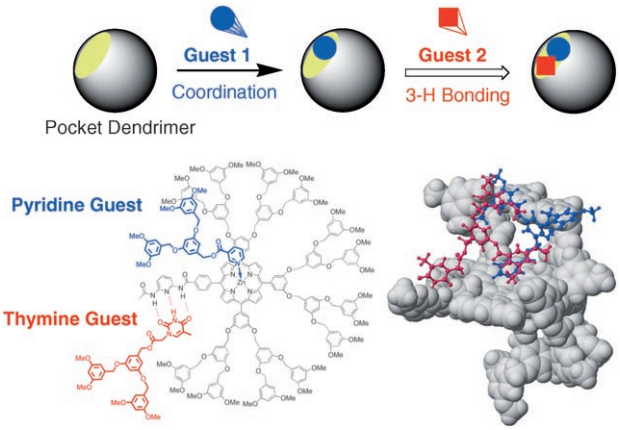

Scheme 1. Bimolecular guest accommodation with pocket dendrimer: zinc coordination plus complementary hydrogen bonding.

[a] Dr. S. Shinoda, M. Ohashi, Prof. Dr. H. Tsukube
Department of Chemistry, Graduate School of Science
Osaka City University, Sugimoto, Sumiyoshi-ku
Osaka 558-8585, (Japan)
Fax: (+81) 6-6605-2560
E-mail: tsukube@sci.osaka-cu.ac.jp

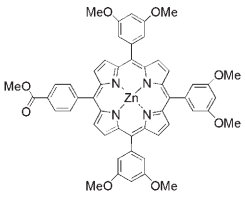

1

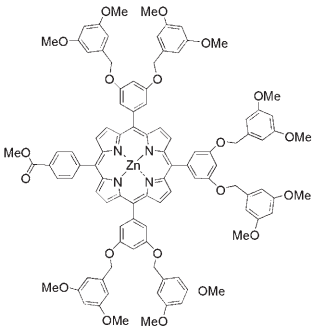

2a

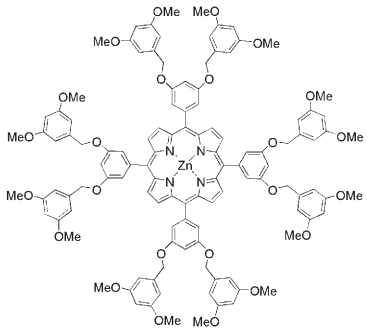

2b

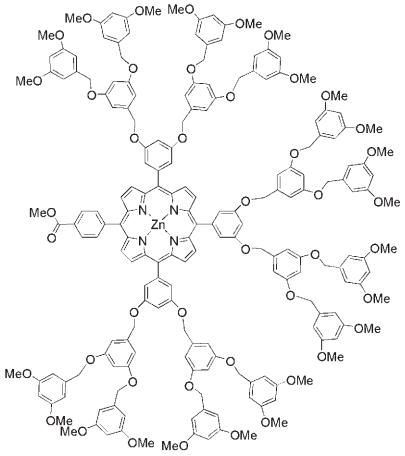

3a

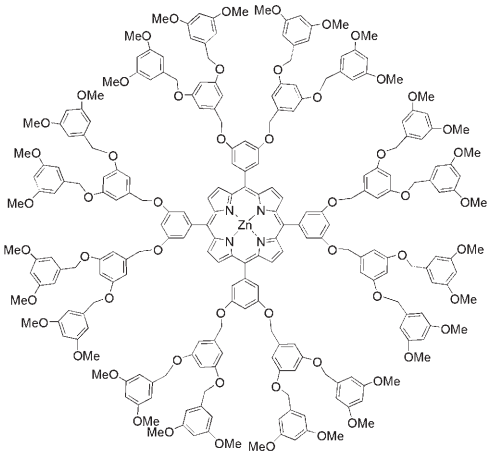

3b

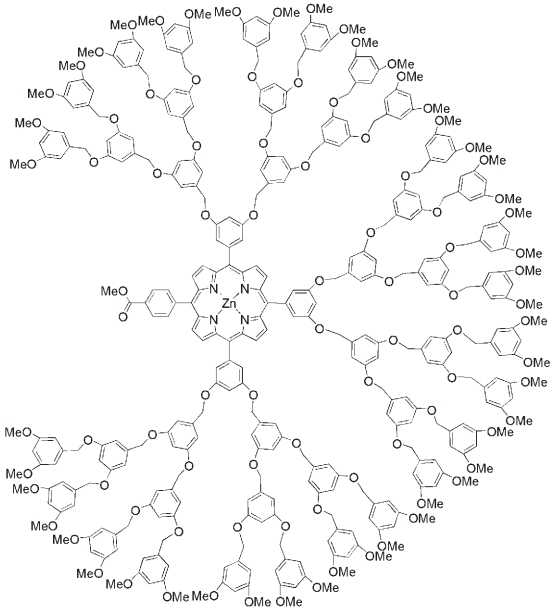

4a

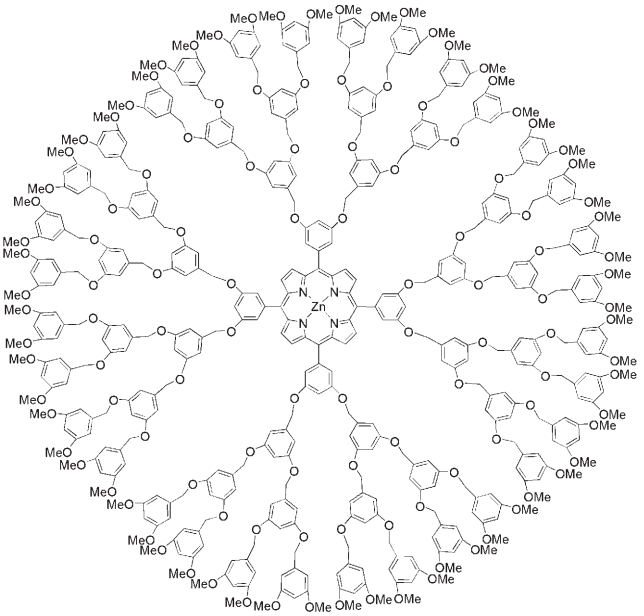

4b

ers catalyzed bimolecular reactions,[8] the number of dendrimers offering bimolecular guest accommodation still remains limited.

We prepared unsymmetrical dendrimer receptors (starting from zinc–porphyrin core **1**) that accommodated two different kinds of guests in the designed nanoscale domains (Scheme 1). A series of unsymmetrical dendrimers **2a**–**4a** were prepared by combining a zinc–porphyrin core with benzyl ether type dendritic substituents. Since one direction of the zinc–porphyrin core was unsubstituted by dendritic

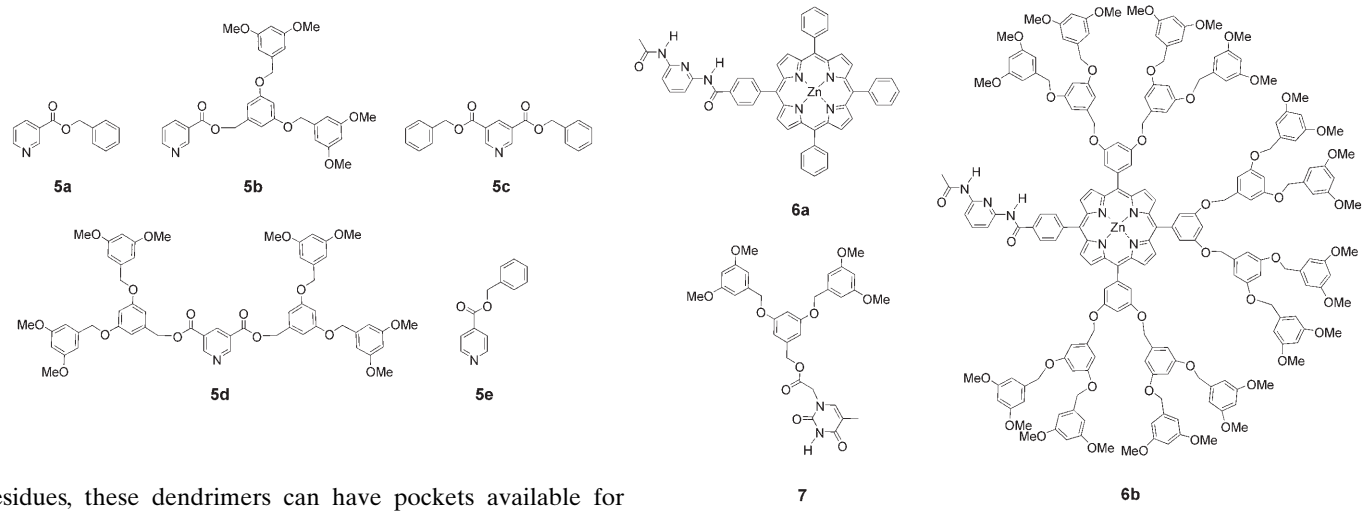

residues, these dendrimers can have pockets available for access of external guests in addition to the zinc–porphyrin centers being available for guest coordination. We compared their receptor functions for several 3- and 4-substituted pyridine derivatives **5a**–**5e** with those of dendrimers **2b**–**4b**. Although their three-dimensional shapes largely depended on the generation, third-generation dendrimer **3a** still had suitable binding abilities for coordinative pyridine derivatives. The diamidopyridine moiety was introduced as a hydrogen-bonding site in the dendrimer pocket (see dendrimer **6b** shown below).[9] The metal coordination and complementary hydrogen-bonding interactions are rather weak, but often involved in biological recognition processes. The present den-

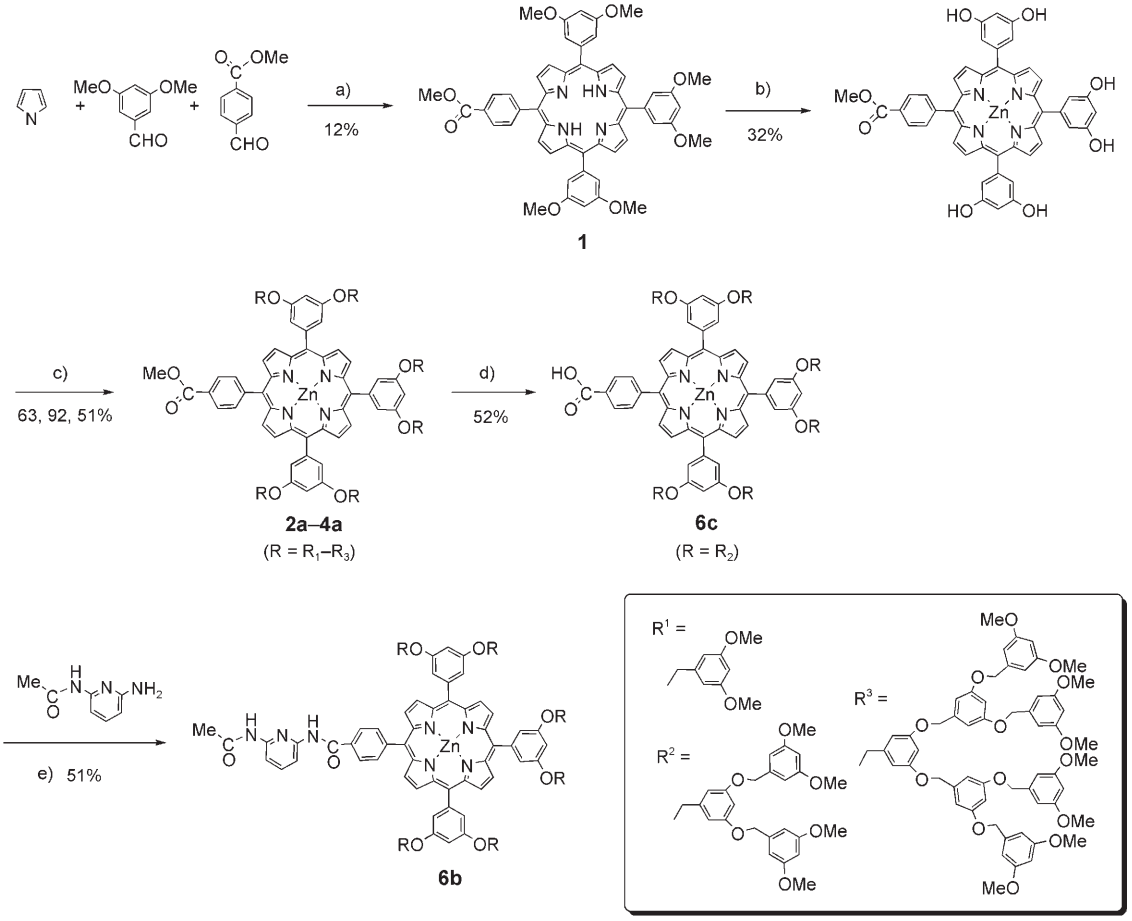

Scheme 2. Synthesis of zinc–porphyrins **1**, **2a**–**4a**, and **6b**. a) $BF_3{\cdot}OEt_2$, $CHCl_3$; then DDQ; b) BBr_3, CH_2Cl_2, 0 °C to RT; then $Zn(OAc)_2$, $CHCl_3$/MeOH, reflux; c) R-OMs, K_2CO_3, [18]crown-6, acetone, 50 °C; d) NaOH, H_2O, THF/MeOH; e) PyBroP®, $(i\text{Pr})_2\text{EtN}$, CH_2Cl_2, RT, 48 h.

drimer receptor **6b** simultaneously bound two kinds of guest substrates **5b** and **7** in its nanoscale domain, and offered a promising strategy for design of bimolecular guest accommodation systems.

Results and Discussion

Synthesis and characterization of pocket dendrimers: Unsymmetrical dendrimers **2a**–**4a** were synthesized by reaction of an A_3B-type tetraphenylporphyrin precursor[7,10] with 7–8 equivalents of benzyl ether type dendritic derivatives,[11] in which six dendritic substituents were attached to the three phenyl groups of the tetraphenylporphyrin core (Scheme 2). Since one phenyl group of each porphyrin core was unsubstituted by dendritic residues, the six attached dendritic substituents partially cover the dendrimer surface leaving a pocket space available for the penetration of external guests. Dendrimer receptor **6b** was prepared by the attachment of diamidopyridine moiety to the porphyrin core of dendrimer **3a**, which formed three hydrogen bonds with complementary thymine guest **7**.[9] As illustrated in Scheme 1, dendrimer **6b** has two different kinds of binding sites to offer bimolecular guest accommodation in the nanoscale domain. Spherical dendrimers **2b**–**4b** were synthesized from A_4-type porphyrin for comparison,[4] in which eight dendritic substituents expanded symmetrically on the dendrimer surfaces. Both types of dendrimers were characterized by UV/Vis, ^{1}H, and ^{13}C NMR spectroscopy, and FAB or MALDI-TOF mass spectrometry as well as by elemental analysis (see Experimental Section).

The dendrimers have high molecular weights and nanoscale diameters:[12] **2a** 1733 and 2.0 nm; **2b** 2008 and 2.0 nm; **3a** 3367 and 3.0 nm; **3b** 4186 and 3.0 nm; **4a** 6635 and 4.0 nm; and **4b** 8533 and 4.0 nm. As illustrated in Figure 1, two dendritic substituents containing outer $-OCH_3(2)$ groups located close to each other and partially occupied the pocket entrance in the fourth-generation dendrimer **4a**, while lower generation dendrimers **2a** and **3a** had open crevice-like spaces. These dendrimers **2a**–**4a** exhibited generation-dependent ^{1}H NMR signals for $-OCH_3$ groups located on the periphery. Dendrimers **3a** and **4a** exhibited two kinds of proton signals for inner $-OCH_3(1)$ and outer $-OCH_3(2)$ groups with an integration ratio of 1:2, but the two $-OCH_3$ signals of dendrimer **2a** apparently overlapped. Dendrimers **3a** and **4a** exhibited similar ^{1}H NMR T_1 values,[4a] but gave larger T_2 values for outer $-OCH_3(2)$ signals than those of inner $-OCH_3(1)$ signals: 0.86 s ($-OCH_3(1)$) < 0.92 s ($-OCH_3(2)$) for **3a**; 0.67 s ($-OCH_3(1)$) < 0.74 s ($-OCH_3(2)$) for **4a**. The observation that the outer $-OCH_3(2)$ group had higher mobility than the inner $-OCH_3(1)$ group suggests that dendrimers **3a** and **4a** have free spaces in the neighborhood of the dendritic substituents containing outer $-OCH_3(2)$ groups.

Pyridine coordination properties of pocket dendrimers 2a–4a: As with spherical dendrimers,[4] guest coordination at

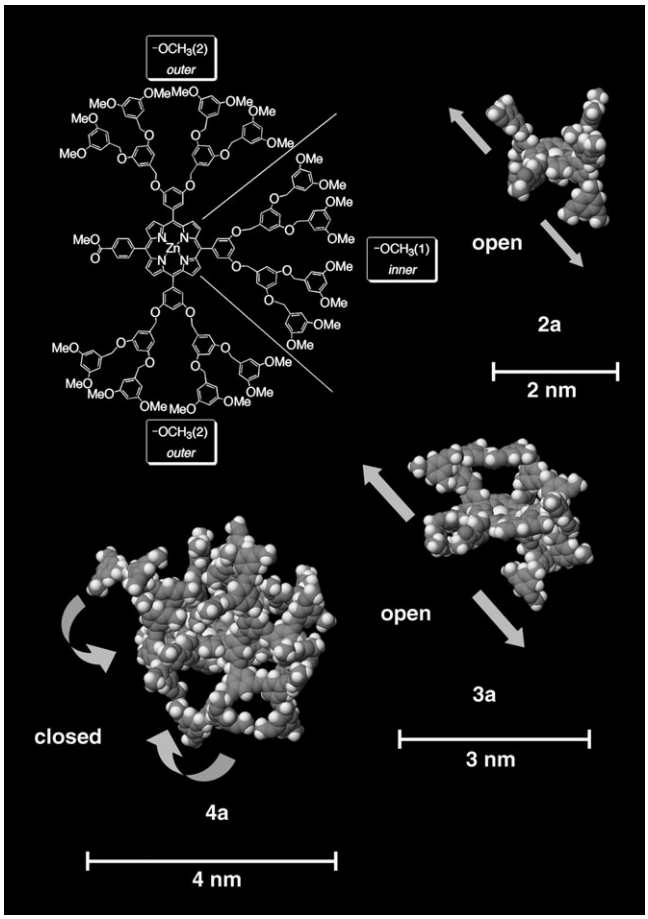

Figure 1. Three-dimensional structures of dendrimers.

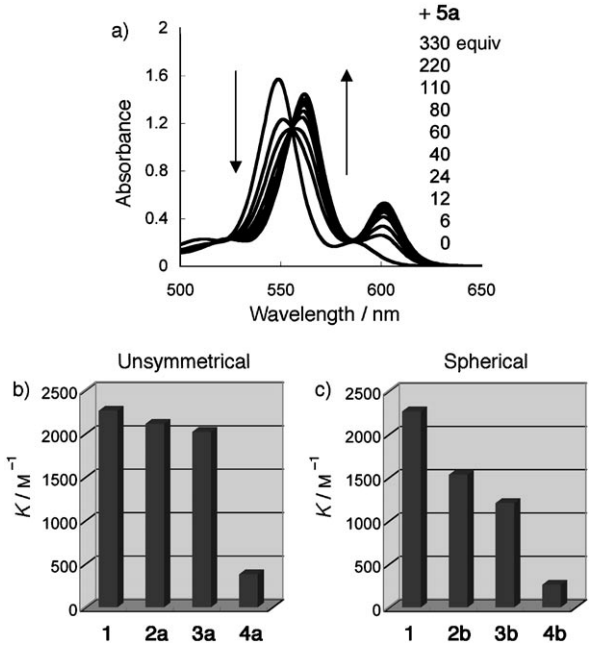

Figure 2. Complexation between pyridine ligands and dendrimers. Absorption spectral changes of dendrimer **3a** upon addition of pyridine guest **5a** (a), and complex stability constants with pyridine guest **5a** for unsymmetrical (b) and spherical (c) dendrimers. Conditions, [**3a**] = 6.00×10^{-5} M in chloroform; 1 cm cuvette; 25 °C.

the axial position of the zinc–porphyrin core of each dendrimer was followed by monitoring absorption spectral changes at the visible (Q) bands. Figure 2 illustrates benzyl nicotinate (**5a**)-induced absorption spectral changes of dendrimer **3a** and compares complex formation constants (K) of **5a** with zinc–porphyrin dendrimers **1**, **2a**–**4a**, and **2b**–**4b**. As the generation of spherical dendrimers increased (**2b**→**4b**), the K values decreased step-by-step: $K=2300$ for **1**, $\geqslant 1500$ for **2b**, >1200 for **3b**, $\geqslant 260\,\text{M}^{-1}$ for **4b**. In particular, benzyl ether clusters of fourth-generation dendrimer **4b** caused severe steric problems in the penetration of pyridine guest **5a**. Similar effects on the guest coordination properties were reported in several zinc–porphyrin dendrimer systems.[4] In contrast, unsymmetrical dendrimers **2a** and **3a** showed almost the same K values to zinc–porphyrin **1**: $K=$ 2300 for **1**, $\cong$2100 for **2a**, $\cong$2000 for **3a**, $\geqslant 380\,\text{M}^{-1}$ for **4a**. Since dendrimer **4a** did not form a stable complex, higher generation dendrimers of this type were ineffective receptors. The third-generation dendrimer **3a** was confirmed to have more effective space for accommodation of pyridine **5a** than corresponding spherical dendrimer **3b**.

Table 1 summarizes complex formation constants for various pyridine guests, which include 3- and 4-substituted and 3,5-disubstituted pyridines **5a–e**. Third-generation dendrimers **3a** and **3b** preferred 3-substituted pyridines **5a** and **5b** to 3,5-disubstituted pyridines **5c** and **5d**. Although dendrimer **3a** bound pyridine **5b** with comparable stability constant to that of zinc–porphyrin **1**, it exhibited higher K value than spherical dendrimer **3b**: $K=1100$ for **1**, $\cong$1100 for **3a**, $>800\,\text{M}^{-1}$ for **3b**. The T_2 values of the two $-OCH_3$ signals of dendrimer **3a** decreased upon complexation with pyridine **5b**: 0.86 s (3.61 ppm) and 0.92 s (3.63 ppm) for $-OCH_3(1)$ and $-OCH_3(2)$, respectively, in the free dendrimer; and 0.77 s (3.66 ppm) and 0.85 s (3.67 ppm), respectively, in the complex form. Each $-OCH_3$ signal appeared as a sharp singlet, indicating that dendritic branches of **3a** and **3b** had no severe steric hindrance. Although the two $-OCH_3$ signals of dendrimer **3a** have a small chemical shift difference, they have high enough resolution to determine the T_2 values. Coordination of pyridine **5b** caused decreases in T_2 values and downfield shifts in both $-OCH_3$ protons. Thus, the coordination of dendritic pyridine **5b** enhanced the residue density on the dendrimer periphery and decreased the mobility of the benzyl ether substituents. When fourth-generation dendrimers **4a** and **4b** were employed, modest K values were estimated for pyridine guest **5b**: $K=210$ for **4a** and $140\,\text{M}^{-1}$ for **4b**. Since dendrimer **4a** gave much lower K value than dendrimer **3a**, the third-generation dendrimer provided the available pocket for pyridine accommodation. 3,5-Disubstituted pyridine derivatives **5c** and **5d** were used as coordinative substrates, but unsymmetrical and spherical dendrimers exhibited slightly different K values: K (with **5c**)$=880$ for **1**, $\geqq 720$ for **3a**, $\geqq 600\,\text{M}^{-1}$ for **3b**. The 4-substituted pyridine **5e** offered somewhat different K values for both types of dendrimers ($K=1100$ for **1**, >860 for **3a**, $>630\,\text{M}^{-1}$ for **3b**). The unsymmetrical third-generation dendrimer **3a** allowed characteristic accommodation of 3-substituted pyridine substrates.

Table 1. Complex formation constants between various dendrimers and pyridines substrates **5a–e**.[a]

	5a	5b	5c	5d	5e
zinc–porphyrin **1**	2300	1100	880	370	1100
dendrimer **3a**	2000	1100	720	310	860
dendrimer **4a**	380	210	[b]	[b]	[b]
dendrimer **3b**	1200	800	600	230	630
dendrimer **4b**	260	140	[b]	[b]	[b]

[a] Determined by titration with visible absorption method. The averaged values of two or more independent experiments are indicated. Reproducibility $<\pm 12\,\%$ (excepting for **5b–4b** and **5e–3b** combinations). [**1** or dendrimer] $=6.00\times10^{-5}$ M, pyridine: 0–300 equiv, 1 cm cuvette, 25 °C. [b] Not determined.

Bimolecular guest accommodation with pocket dendrimer 6b: A new dendrimer receptor of the third-generation **6b** was designed for bimolecular guest accommodation, which had a diamidopyridine unit as an additional hydrogen-bonding site in the pocket. The diamidopyridine compounds were reported to form three-point hydrogen-bonding interactions with thymine derivatives.[9] When dendritic thymine **7** was added to a solution of dendrimer **6b** in $CDCl_3$, complementary hydrogen-bond formation was monitored by ^{1}H NMR spectroscopy. As illustrated in Figure 3a–e, the signals for $-$NH protons of both dendrimer **6b** and guest **7** shifted in the lower field direction upon complexation. Since the two proton signals (labeled 1 and 2 in Figure 3) of the dendrimer **6b** moved dramatically, stability constant K of the resulting hydrogen-bonding complex was determined by monitoring them. Dendrimer **6b** exhibited comparable K value for thymine derivative **7** to that with zinc–porphyrin **6a**: $K=170$ for **6b** and $210\,\text{M}^{-1}$ for **6a**. The curve-fitting calculation also indicated that the signal 1 for one amide proton of dendrimer **6b** completely complexed with thymine **7** was recorded at $\delta=10.49$ ppm. This means that 69 % of dendrimer **6b** was typically estimated to form a hydrogen-bonding complex in the presence of five equivalents of thymine **7** (see Figure 3d). Under the same conditions, the $-OCH_3$ protons of dendrimer **6b** exhibited similar NMR T_2 and chemical shift values to those of free dendrimer: 0.85 s and 3.64 ppm for $-OCH_3(1)$, and 0.86 s and 3.65 ppm for $-OCH_3(2)$ in the free dendrimer **6b**; 0.84 s and 3.61 ppm for $-OCH_3(1)$, and 0.84 s and 3.63 ppm for $-OCH_3(2)$ in dendrimer **6b** + thymine **7**. The terminal $-OCH_3$ protons of thymine **7** appeared as a singlet, suggesting that exchange between the bound and unbound states occurred more rapidly than the NMR timescale, and its phenyl rings freely rotated around C–C single bonds even at the bound state. Thus, third-generation dendrimer **6b** binding thymine derivative **7** can have high flexibility, enough to accommodate the second guest in its nanoscale domain.

To demonstrate bimolecular guest accommodation with dendrimer **6b**, the diluted solution of dendrimer **6b** (0.60 mM) in $CDCl_3$ was characterized by ^{1}H NMR and ab-

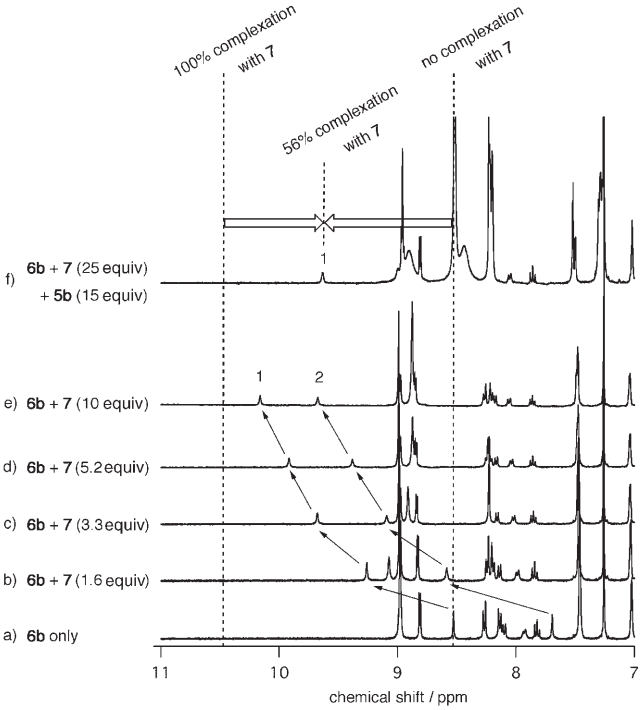

Figure 3. ^{1}H NMR spectral changes of dendrimer **6b** induced by complementary hydrogen-bond formation and subsequent pyridine coordination. [dendrimer **6b**]/[thymine guest **7**]/[pyridine guest **5b**]: a) 3.0/0/0 mM; b) 3.0/4.7/0 mM; c) 3.0/10/0 mM; d) 3.0/15/0 mM; e) 3.0/30/0 mM; f) 0.60/15/9.0 mM (in this case the diluted concentration of **6b** was used).

sorption spectroscopy. Although zinc–porphyrin **6a** exhibited concentration-dependent amide proton signals due to the self-association, sterically bulky dendrimer **6b** was confirmed to give the amide protons at the fixed chemical shifts. Figure 3f illustrates ^{1}H NMR spectrum of a mixture of dendrimer **6b** (0.60 mM), thymine **7** (15.0 mM), and pyridine **5b** (9.0 mM). Since the amide signal 1 of dendrimer **6b** appeared at $\delta = 9.63$ ppm, 56% of dendrimer **6b** formed three-point hydrogen bonds with thymine guest **7**. The absorption spectrum of this ternary mixture also revealed about 90% of the dendrimer bound pyridine **5b**, indicating that dendrimer receptor **6b** simultaneously accommodated thymine **7** and pyridine **5b** in its single domain.[13] When benzyl nicotinate **5a** was used instead of dendritic pyridine **5b**, 90% of dendrimer **6b** bound pyridine **5a** and 57% of dendrimer **6b** accommodated thymine derivative **7**. Since a combination of **6a**, **7**, and **5b** gave similar spectral profiles, dendrimer **6b** offered suitable space for bimolecular guest accommodation.

Conclusion

The present type of unsymmetrical dendrimers was demonstrated to provide nanoscale platforms for design of bimolecular guest binding receptors. Among the unsymmetric dendrimers, third-generation ones composed of a zinc–porphyrin core, benzyl ether dendritic moieties, and a diamidopyridine unit realized bimolecular guest accommodation, in which zinc coordination and complementary hydrogen-bonding sites operated independently. Further structural sophistication of the unsymmetrical dendrimers can allow protein-like recognition and enzyme-like catalysis.

Experimental Section

Synthesis of pocket dendrimers 2a–4a: As illustrated in Scheme 2, unsymmetric dendrimers **2a**–**4a** were synthesized by reactions of A_3B-type tetraphenylporphyrin precursor with excess of benzyl ether dendritic derivatives.

Dendrimer 2a: This dendrimer was prepared by reaction of [5-(4-methoxycarbonylphenyl)-10,15,20-tris(3,5-dihydroxyphenyl)porphinato]zinc-(II)[7] (79 mg, 0.095 mmol) and the corresponding mesylate (164 mg, 0.67 mmol) in the presence of anhydrous K_2CO_3 (131 mg, 0.95 mmol) and [18]crown-6 (20 mg, 0.076 mmol) in dried acetone (25 mL). The reaction mixture was protected from light by using aluminum foil and stirred at 50 °C under an N_2 atmosphere. After the reaction was complete (24 h), the solvents were removed in vacuo, and the residue was dissolved in dichloromethane (30 mL), filtered, and washed with dichloromethane. The filtrate and washings were combined and evaporated. To the stirred solution of the residue dissolved in a minimum amount of dichloromethane (ca. 5 mL) was added methanol (ca. 30 mL), and the formed precipitate was collected by filtration. Silica gel chromatography with 5% ethyl acetate in dichloromethane as eluent gave **2a** as purple solid in a 63% yield. M.p. 100–102 °C; ^{1}H NMR (300 MHz, $CDCl_3$): $\delta = 3.76$ (s, 36H; OMe), 4.09 (s, 3H; CO_2Me), 5.15 (s, 12H; $H^{c,c'}$), 6.41 (t, $^4J(H,H) = 2.2$ Hz, 6H; $H^{a,a'}$), 6.63 (d, $^4J(H,H) = 2.0$ Hz, 12H; $H^{b,b'}$), 7.04 (m, 3H; $H^{d,d'}$), 7.49 (m, 6H; $H^{e,e'}$), 8.30 (d, $^3J(H,H) = 8.4$ Hz, 2H; H^{forg}), 8.42 (d, $^3J(H,H) = 8.3$ Hz, 2H; H^{forg}), 8.84 (d, $^3J(H,H) = 4.8$ Hz, 2H; pyrrole-β), 8.98 (s, 4H; pyrrole-β), 9.00 ppm (d, $^3J(H,H) = 8.3$ Hz, 2H; pyrrole-β); ^{13}C NMR (75 MHz, $CDCl_3$): $\delta = 52.53$, 55.48, 70.41, 100.18, 102.10, 105.50, 115.24, 121.04, 127.90, 129.48, 131.64, 132.26, 132.39, 134.55, 139.27, 144.63, 144.67, 147.87, 149.69, 150.02, 150.21, 157.93, 161.16, 167.52 ppm; IR (film between KBr discs): $\tilde{\nu} = 1718$ cm^{-1} (C=O); MS (FAB): m/z: 1730.5 $[M]^+$; elemental analysis calcd (%) for $C_{100}H_{90}N_4O_{20}Zn$: C 69.30, H 5.23, N 3.23; found: C 69.20, H 5.20, N 3.17.

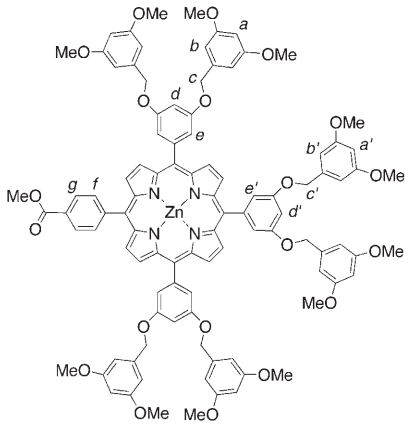

Dendrimers 3a and 4a: These dendrimers were similarly prepared and finally purified by gel permeation chromatography with a 1H-2H JAIGEL preparative column (Nihon Bunseki Kogyo Ltd., Tokyo) and chloroform as the eluent.

Data for 3a: Purple crystalline solid in 92% yield. ^{1}H NMR (400 MHz, $CDCl_3$): δ=3.62 (s, 24H; OMe′), 3.64 (s, 48H; OMe), 4.11 (s, 3H; CO_2Me), 4.91 (brs, 8H; H$^{c'}$), 4.92 (brs, 16H; H^{c}), 5.12 (brs, 4H; H^{f}),

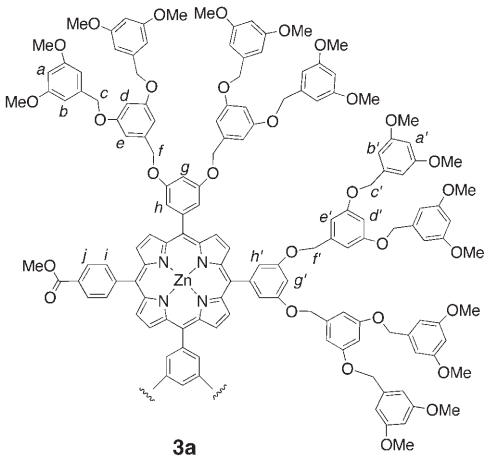

3a

5.14 (brs, 8H; H^{f}), 6.24 (t, ^4J(H,H)=2.2 Hz, 4H; H$^{a'}$), 6.27 (t, ^4J(H,H)=2.2 Hz, 8H; H^{a}), 6.44 (d, ^4J(H,H)=2.2 Hz, 8H; H$^{b'}$), 6.46 (d, ^4J(H,H)=2.2 Hz, 16H; H^{b}), 6.55 (brt, ^4J(H,H)=2.0 Hz, 6H; H$^{d,d'}$), 6.73 (brd, ^4J(H,H)=2.0 Hz, 12H; H$^{e,e'}$), 7.03 (brt, ^4J(H,H)=2.1 Hz, 3H; H$^{g,g'}$), 7.45 (d, ^4J(H,H)=2.2 Hz, 2H; H$^{h'}$), 7.47 (d, ^4J(H,H)=2.2 Hz, 4H; H^{h}), 8.23 (d, ^3J(H,H)=8.1 Hz, 2H; H$^{i\text{or}j}$), 8.39 (d, ^3J(H,H)=8.3 Hz, 2H; H$^{i\text{or}j}$), 8.82 (d, ^3J(H,H)=4.9 Hz, 2H; pyrrole-β), 8.97–8.99 (m, 6H; pyrrole-β), 8.98 ppm (d, ^3J(H,H)=4.9 Hz, 2H; pyrrole-β); ^{13}C NMR (75 MHz, $CDCl_3$): δ=52.27, 55.17, 55.19, 69.98, 70.22, 99.82, 101.71, 101.91, 105.12, 106.51, 115.09, 119.54, 120.74, 120.80, 127.66, 129.14, 131.45, 132.06, 132.14, 134.39, 139.00, 139.20, 144.63, 147.76, 149.49, 149.81, 149.99, 150.00, 157.75, 160.04, 160.80, 167.30 ppm; IR (film between KBr discs): $\tilde{\nu}$=1718 cm^{-1} (C=O); MS (FAB): m/z: 3363.7 $[M]^+$; elemental analysis calcd (%) for $C_{196}H_{186}N_4O_{44}Zn$: C 69.92, H 5.57, N 1.66; found: C 69.82, H 5.55, N 1.60.

Data for 4a: Purple crystalline solid in 51% yield. ^{1}H NMR (400 MHz, $CDCl_3$): δ=3.57 (s, 48H; OMe′), 3.61 (s, 96H; OMe), 4.08 (s, 3H; CO_2Me), 4.72 (s, 16H; H$^{c'}$), 4.79 (s, 32H; H^{c}), 4.87 (s, 8H; H$^{f'}$), 4.90 (s, 16H; H^{f}), 5.11 (brs, 12H; H$^{i',j}$), 6.19 (brt, ^4J(H,H)=2.1 Hz, 8H; H$^{a'}$), 6.23

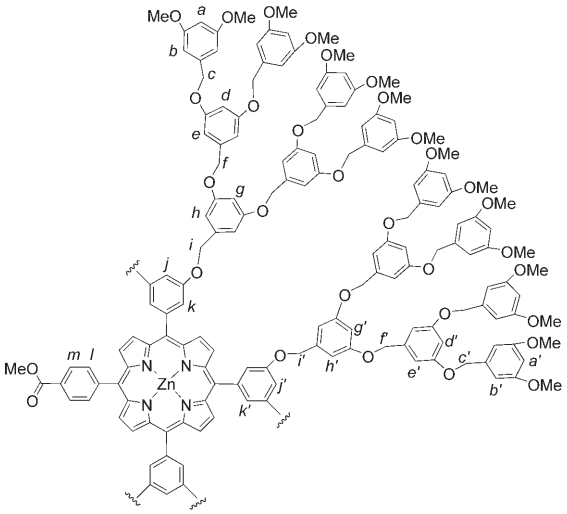

4a

(brt, ^4J(H,H)=2.0 Hz, 16H; H^{a}), 6.33 (brd, ^4J(H,H)=2.0 Hz, 16H; H$^{b'}$), 6.38 (bm, 36H; H$^{b,d'}$), 6.44 (brt, ^4J(H,H)=2.1 Hz, 8H; H^{d}), 6.53–6.54 (bm, 14H; H$^{e,g,g'}$), 6.57 (brd, ^4J(H,H)=2.0 Hz, 16H; H^{e}), 6.70 (brd, ^4J(H,H)=1.2 Hz, 4H; H$^{h'}$), 6.72 (brd, ^4J(H,H)=1.5 Hz, 8H; H^{h}), 7.02 (brs, 3H; H$^{j,f'}$), 7.46 (s, 2H; H$^{k'}$), 7.48 (s, 4H; H^{k}), 8.23 (d, 2H; ^3J(H,H)=8.1 Hz, H$^{l\text{or}m}$), 8.38 (d, ^3J(H,H)=8.1 Hz, 2H; H$^{l\text{or}m}$), 8.79 (d, ^3J(H,H)=4.6 Hz, 2H; pyrrole-β), 8.93–8.95 (m, 4H; pyrrole-β), 8.98 ppm (d, ^3J(H,H)=4.6 Hz, 2H; pyrrole-β); ^{13}C NMR (100 MHz, $CDCl_3$): δ=52.29, 55.11, 55.15, 69.77, 69.83, 70.08, 99.69, 99.75, 101.51, 101.71, 105.07, 106.14, 106.19, 106.40, 106.48, 115.24, 115.36, 119.42, 120.61, 120.69, 127.66, 129.15, 131.36, 132.02, 134.46, 138.92, 138.94, 139.19, 139.28, 139.36, 144.63, 144.70, 147.85, 149.36, 149.68, 149.86, 157.72, 159.90, 159.93, 160.05, 160.68, 160.74 ppm; IR (film between KBr discs): $\tilde{\nu}$=1718 cm^{-1} (C=O); MS (MALDI-TOF, reflectron mode): m/z: 6634.6 $[M]^+$; elemental analysis calcd (%) for $C_{388}H_{378}N_4O_{92}Zn$: C 70.24, H 5.74, N 0.84; found: C 70.07, H 5.73, N 0.79.

Spherical dendrimers 2b–4b: These dendrimers were synthesized by the reported methods.[4a] (See the above shown structure drawings of the corresponding unsymmetrical dendrimers for the NMR assignments.)

Data for 2b: Purple crystals in 25% yield. ^{1}H NMR (300 MHz, $CDCl_3$): δ=3.76 (s, 48H; OMe), 5.16 (s, 16H; H^{c}), 6.42 (t, ^4J(H,H)=2.1 Hz, 8H; H^{a}), 6.64 (d, ^4J(H,H)=2.4 Hz, 16H; H^{b}), 7.04 (t, ^4J(H,H)=2.3 Hz, 4H; H^{d}), 7.50 (d, ^4J(H,H)=2.1 Hz, 8H; H^{e}), 8.97 ppm (s, 8H; pyrrole-β); ^{13}C NMR (100 MHz, $CDCl_3$): δ=55.36, 70.30, 100.08, 101.96, 105.38, 115.10, 120.69, 131.97, 139.18, 144.64, 149.94, 157.82, 161.05 ppm; MS (FAB): m/z: 2004.7 $[M]^+$; elemental analysis calcd (%) for $C_{116}H_{108}N_4O_{24}Zn$: C 69.40, H 5.42, N 2.79; found: C 69.23, H 5.40, N 2.58.

Data for 3b: Purple crystalline solid in 26% yield. ^{1}H NMR (400 MHz, $CDCl_3$): δ=3.62 (s, 96H; OMe), 4.91 (s, 32H; H^{c}), 5.12 (s, 16H; H^{f}), 6.26 (t, ^4J(H,H)=2.2 Hz, 16H; H^{a}), 6.45 (d, ^4J(H,H)=2.4 Hz, 32H; H^{b}), 6.54 (t, ^4J(H,H)=2.0 Hz, 8H; H^{d}), 6.73 (d, ^4J(H,H)=2.2 Hz, 16H; H^{e}), 7.03 (t, ^4J(H,H)=2.3 Hz, 4H; H^{g}), 7.46 (d, ^4J(H,H)=2.0 Hz, 8H; H^{h}), 8.97 ppm (s, 8H; pyrrole-β); ^{13}C NMR (75 MHz, $CDCl_3$): δ=55.20, 70.03, 70.26, 99.86, 101.74, 101.87, 105.15, 106.56, 115.05, 120.60, 131.92, 139.05, 139.26, 144.73, 149.89, 157.78, 160.09, 160.84 ppm; MS (FAB): m/z: 4181.4 $[M]^+$; elemental analysis calcd (%) for $C_{244}H_{236}N_4O_{56}Zn$: C 70.01, H 5.68, N 1.34; found: C 69.97, H 5.70, N 1.33.

Data for 4b: Purple crystalline solid in 30% yield. ^{1}H NMR (300 MHz, $CDCl_3$): δ=3.58 (s, 192H; OMe), 4.75 (s, 64H; H^{c}), 4.86 (s,32H; H^{f}), 5.08 (s, 16H; H^{i}), 6.21 (brs, 32H; H^{a}), 6.36 (d, ^4J(H,H)=1.7 Hz, 64H; H^{b}), 6.41 (brs, 16H; H^{d}), 6.52 (brs, 8H; H^{g}), 6.54 (brs, 32H; H^{e}), 6.70 (brs, 16H; H^{h}), 7.01 (brs, 4H; H^{j}), 7.48 (brs, 8H; H^{k}), 8.95 ppm (s, 8H; pyrrole-β); MS (MALDI-TOF, reflectron mode): m/z: 8542.1 $[M]^+$; elemental analysis calcd (%) for $C_{500}H_{492}N_4O_{120}Zn$: C 70.30, H 5.81, N 0.66; found: C 70.03, H 5.80, N 0.71.

Synthesis of pyridine ligands—general preparation described for 3,5-bis(3,5-dimethoxybenzyloxy)benzyl nicotinate (5b): The pyridine ligands were prepared from nicotinoyl chloride and the corresponding alcohol.[14] For **5b** 3,5-bis(3,5-dimethoxybenzyloxy)benzyl alcohol (543 mg, 1.23 mmol) was added to a stirred solution of nicotinoyl chloride hydrochloride (200 mg, 1.12 mmol) and triethylamine (0.18 mL, 2.46 mmol) in dichloromethane (10 mL) at 0°C. After overnight stirring at room temperature, the mixture was washed with 5% HCl (7 mL) and with brine until the solution became neutral. The dichloromethane layer was dried over anhydrous Na_2SO_4 and concentrated. The brown solid was purified by silica-gel chromatography using 45% ethyl acetate in dichloromethane as eluent, then was recrystallized from dichloromethane/diethyl ether in 63% yield. M.p. 100–102°C; ^{1}H NMR (300 MHz, $CDCl_3$): δ=3.79 (s, 12H; OMe), 4.98 (s, 4H; benzylic-CH_2), 5.31 (s, 2H; benzylic-CH_2), 6.41 (t, ^4J(H,H)=2.1 Hz, 2H; ArH), 6.56–6.60 (m, 5H; ArH), 6.67 (d, ^4J(H,H)=2.0 Hz, 2H; ArH), 7.40 (m, 1H; pyridine-5-H), 8.30 (m, 1H; pyridine-4-H), 8.79 (m, 1H; pyridine-6-H), 9.26 ppm (d, ^4J(H,H)=2.2 Hz, 1H; pyridine-2-H); ^{13}C NMR (100 MHz, $CDCl_3$): δ=55.38, 66.93, 70.13, 99.97, 101.97, 105.24, 107.24, 123.32, 125.96, 137.17, 137.77, 139.01, 151.07, 153.58, 160.10, 161.03, 165.07 ppm; MS (FAB): m/z: 546.2 $[M+H]^+$; elemental analysis calcd (%) for $C_{31}H_{31}NO_8$: C 68.25, H 5.73, N 2.57; found: C 68.17, H 5.71, N 2.48.

Data for 5c: Brown solid in 67%. ^{1}H NMR (300 MHz, $CDCl_3$): $\delta=5.42$ (s, 4H; benzylic-CH_2), 7.37–7.47 (m, 10H; ArH), 8.89–8.90 (m, 1H; pyridine-4-H), 9.39–9.39 ppm (m, 2H; pyridine-2,6-H); ^{13}C NMR (100 MHz, $CDCl_3$): $\delta=67.49$, 126.02, 128.44, 128.63, 128.72, 135.18, 138.17, 154.36, 164.27 ppm; IR (film between KBr discs): $\tilde{\nu}=1728\ cm^{-1}$ (C=O); MS (FAB): m/z: 348.1 $[M+H]^+$; elemental analysis calcd (%) for $C_{21}H_{17}NO_4$: C 72.61, H 4.93, N 4.03; found: C 72.55, H 4.85, N 4.00.

Data for 5d: Brown solid in 78%. m.p. 69–71°C; ^{1}H NMR (300 MHz, $CDCl_3$): $\delta=3.78$ (s, 24H; OMe), 4.97 (s, 8H; benzylic-CH_2), 5.34 (s, 4H; benzylic-CH_2), 6.39 (t, ^4J(H,H)=2.3 Hz, 4H; ArH), 6.56 (d, ^4J(H,H)=2.2 Hz, 8H; ArH), 6.58 (t, ^4J(H,H)=2.1 Hz, 2H; ArH), 6.66 (d, ^4J(H,H)=2.0 Hz, 4H; ArH), 8.89–8.90 (m, 1H; pyridine-4-H), 9.37–9.38 ppm (m, 2H; pyridine-2,6-H); ^{13}C NMR (100 MHz, $CDCl_3$): $\delta=$ 55.36, 67.34, 70.13, 99.97, 102.15, 105.23, 107.40, 126.07, 137.45, 138.34, 138.98, 154.27, 160.12, 161.02, 164.19 ppm; IR (film between KBr disc): $\tilde{\nu}=1728\ cm^{-1}$ (C=O); MS (FAB): m/z: 1011.7 $[M]^+$; elemental analysis calcd (%) for $C_{57}H_{57}NO_{16}$: C 67.65, H 5.68, N 1.38; found: C 67.87, H 5.65, N 1.35.

Synthesis of diamidopyridine-functionalized zinc–porphyrin 6a: A solution of 2-amino-6-acetamidopyridine (54 mg, 0.36 mmol),[15] [5-(4-carboxyphenyl)-10,15,20-triphenylporphinato]zinc(II) (130 mg, 0.18 mmol),[7]

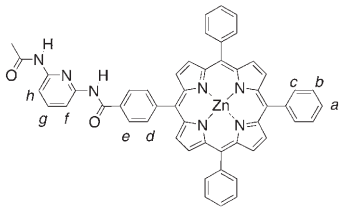

6a

and bromo-tris(pyrrolidino)phosphonium hexafluorophosphate (PyBroP, 126 mg, 0.27 mmol) as a coupling reagent in dichloromethane (20 mL) was treated with *N*,*N*-diisopropylethylamine (DIEA, 0.54 mmol) under stirring at 0°C. The ice bath was removed after 1 min and the stirring continued at room temperature for 48 h. The reaction mixture was concentrated and the residue dissolved in ethyl acetate. This was then washed with water and dried over anhydrous Na_2SO_4. The crude product was purified by silica-gel chromatography with dichloromethane and ethyl acetate (0%–10%) as eluent. The fifth band fraction was further subjected to preparative thin-layer chromatography on silica gel with 35% hexane and 10% methanol in CH_2Cl_2. Recrystallization from dichloromethane/methanol gave **6a** as purple crystalline solid in 41% yield. M.p. 249–251°C; ^{1}H NMR (400 MHz, $CDCl_3$, [**6a**]=3.0 мм): $\delta=$ 2.17 (s, 3H; CH_3), 7.59 (s, 1H; CONH), 7.7–7.9 (m, 11H; $H^{a,b,g,for\,h}$), 8.16 (d, ^3J(H,H)=7.6 Hz, 1H; $H^{for\,h}$), 8.22 (m, 6H; Ar), 8.23 (2H; d, H^c), 8.37 (2H; d, ^3J(H,H)=8.0 Hz, H^d), 8.54 (s, 1H; CONH), 8.89 (d, ^3J(H,H)= 4.8 Hz, 2H; pyrrole-β), 8.96 (s, 4H; pyrrole-β), 8.98 ppm (d, ^3J(H,H)= 4.8 Hz, 2H; pyrrole-β); ^{13}C NMR (100 MHz, $CDCl_3$): $\delta=24.45$, 109.58, 109.67, 119.06, 121.36, 121.58, 125.26, 126.58, 127.56, 131.39, 132.13, 132.21, 132.36, 132.99, 134.43, 134.79, 140.97, 142.74, 147.33, 149.29, 149.45, 149.53, 150.21, 150.34, 150.41, 165.42, 168.28 ppm; IR (film between KBr discs): $\tilde{\nu}=1683\ cm^{-1}$ (C=O); MS (FAB): m/z: 853.2 $[M]^+$; elemental analysis calcd (%) for $C_{52}H_{35}N_7O_2Zn+H_2O$: C 71.52, H 4.27, N 11.23; found: C 71.25, H 4.08, N 10.95.

Synthesis of diamidopyridine-functionalized dendrimer 6b via precursor 6c

Preparation of ***6c***: Dendrimer **3a** (225 mg, 0.067 mmol) was dissolved in THF (8 mL) and methanol (3 mL). Aqueous NaOH solution (91 mg, 2.3 mmol/1.0 mL) was added and the reaction mixture was protected from light and stirred at room temperature (12 h). The solvent were removed in vacuo, and the residue was dissolved in dichloromethane and washed with water (2×10 mL), 2% citric acid (10 mL) and then with water (2×10 mL). The organic layer was separated, dried over $MgSO_4$, filtered, and evaporated. The residue was purified by silica-gel chromatography using acetone and then 10% methanol in acetone to give dendrimer precursor **6c** in 52% yield. This was used in next amidation just after the disappearance of CO_2Me proton signals in its ^{1}H NMR spectrum. ^{1}H NMR (400 MHz, $CDCl_3$): $\delta=3.60$ (s, 24H; OMe′), 3.62 (s, 48H; OMe), 4.87 (brs, 24H; $H^{c,c'}$), 5.10 (brs, 12H; $H^{f,f'}$), 6.24 (m, 12H; $H^{a,a'}$), 6.42 (m, 24H; $H^{b,b'}$), 6.51 (brs, 6H; $H^{d,d'}$), 6.70 (brs, 12H; $H^{e,e'}$), 7.02 (brs, 3H; $H^{g,g'}$), 7.48 (brs, 6H; $H^{h,h'}$), 8.28 (d, ^3J(H,H)=8.1 Hz, 2H; $H^{i\,or\,j}$), 8.42 (d, ^3J(H,H)=8.3 Hz, 2H; $H^{i\,or\,j}$), 8.84 (d, ^3J(H,H)=4.9 Hz, 2H; pyrrole-β), 8.99 (m, 4H; pyrrole-β), 9.01 ppm (d, ^3J(H,H)=4.9 Hz, 2H; pyrrole-β); IR (film between KBr discs): $\tilde{\nu}=1712\ cm^{-1}$ (C=O).

Preparation of ***6b***: A solution of 2-amino-6-acetamidopyridine (32 mg, 0.21 mmol), dendrimer precursor **6c** (141 mg, 0.042 mmol), and PyBroP (29 mg, 0.063 mmol) as a coupling reagent in dichloromethane (15 mL)

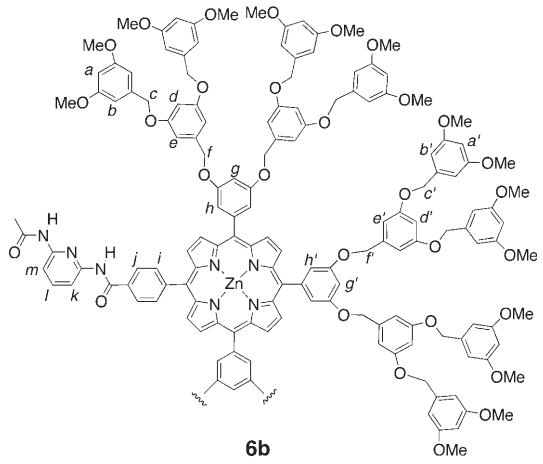

6b

was stirred with DIEA (0.020 mmol) at 0°C. The ice bath was removed after 1 min and the stirring was continued at room temperature for 18 h. The reaction mixture was treated in a similar manner to **6a**, and finally purified by preparative thin-layer chromatography (PLC) on silica gel with 35% hexane and 10% methanol in dichloromethane as eluent. The recrystallization from dichloromethane/hexane offered **6b** as purple crystalline solid in 51% yield. M.p. 79–81°C; ^{1}H NMR (400 MHz, $CDCl_3$): $\delta=2.19$ (s, 3H; $COCH_3$), 3.61 (s, 24H; OMe′), 3.63 (s, 48H; OMe), 4.89 (brs, 24H; $H^{c,c'}$), 5.12 (brs, 12H; $H^{f,f'}$), 6.24 (t, ^4J(H,H)=2.2 Hz, 4H; $H^{a'}$), 6.25 (t, ^4J(H,H)=2.1 Hz, 8H; H^a), 6.43 (d, ^4J(H,H)=2.2 Hz, 8H; $H^{b'}$), 6.44 (d, ^4J(H,H)=2.0 Hz, 16H; H^b), 6.53 (brs, 6H; $H^{d,d'}$), 6.71 (brs, 12H; $H^{e,e'}$), 7.02 (brs, 3H; $H^{g,g'}$), 7.46 (d, ^4J(H,H)=2.2 Hz, 6H; $H^{h,h'}$), 7.69 (s, 1H; CONH), 7.82 (t, ^3J(H,H)=7.8 Hz, 1H; H^l), 7.93 (brd, ^3J(H,H)= 7.1 Hz, 1H; $H^{k\,or\,m}$), 8.10 (d, ^3J(H,H)=8.1 Hz, 1H; $H^{k\,or\,m}$) 8.13 (d, ^3J(H,H)=8.0 Hz, 2H; $H^{i\,or\,j}$), 8.26 (d, ^3J(H,H)=8.1 Hz, 2H; $H^{i\,or\,j}$), 8.53 (s, 1H; CONH), 8.81 (d, ^3J(H,H)=4.4 Hz, 2H; pyrrole-β), 8.97–8.99 ppm (m, 6H; pyrrole-β); ^{13}C NMR (100 MHz, $CDCl_3$): $\delta=24.60$, 55.18, 55.21, 69.98, 70.22, 99.84, 101.70, 101.70, 101.89, 105.14, 106.51, 109.65, 115.10, 115.15, 119.14, 120.76, 120.88, 125.24, 131.35, 132.06, 132.11, 132.21, 132.96, 134.72, 139.00, 139.22, 140.94, 144.62, 147.20, 149.45, 149.49, 149.57, 149.80, 150.00, 150.04, 157.73, 160.05, 160.80, 165.52, 168.44 ppm; IR (film between KBr discs): $\tilde{\nu}=1682\ cm^{-1}$ (C=O); MS (FAB): m/z: 3482.6 $[M]^+$; elemental analysis calcd (%) for: $C_{202}H_{191}N_7O_{44}Zn$: C 69.60, H 5.52, N 2.81; found: C 69.88, H 5.77, N 2.72.

Synthesis of thymine derivative 7: Thymine-1-acetic acid (100 mg, 0.54 mmol), *N*,*N*-dicyclohexylcarbodiimide (DCC, 121 mg, 0.59 mmol), and 1-hydroxybenzotriazole (HOBt, 80 mg, 0.59 mmol) were added to dry DMF (30 mL) and stirred at 0°C for 30 min; then 3,5-bis(3,5-dimethoxybenzyloxy)benzyl alcohol (261 mg, 0.59 mmol) was added. After stirring for 30 h, the precipitate of urea was filtered off, and the filtrate was concentrated under reduced pressure. The residue was dissolved in ethyl acetate, filtered off to remove the urea, and washed with water (20 mL) and brine (20 mL). The organic layer was separated, dried over $MgSO_4$, filtered, and evaporated. Recrystallization from dichlorome-

thane/diethyl ether gave **7** as white powder in 78% yield. M.p. 67–71°C; ^{1}H NMR (400 MHz, $CDCl_3$): $\delta = 1.93$ (s, 3H; CH_3), 3.80 (s, 12H; OMe), 4.45 (s, 2H; CH_2), 4.98 (s, 4H; benzylic-CH_2), 5.14 (s, 2H; benzylic-CH_2), 6.42 (t, ^4J(H,H) = 2.2 Hz, 2H; outer ArH), 6.57 (d, ^4J(H,H) = 2.0 Hz, 7H; ArH), 6.92 (s, 1H; NH), 8.18 ppm (s, 1H; thymine-CH); ^{13}C NMR (100 MHz, $CDCl_3$): $\delta = 12.27$, 48.63, 55.36, 67.54, 70.07, 99.90, 102.26, 105.27, 107.22, 111.27, 136.98, 139.02, 140.04, 150.63, 160.05, 161.00, 163.78, 167.34 ppm; IR (film between KBr discs): $\tilde{\nu} = 1685$, 1750 cm^{-1} (C=O); MS (FAB): m/z: 607.1 $[M+H]^+$; elemental analysis calcd (%) for: $C_{32}H_{34}N_2O_{10}\cdot(H_2O)_{0.5}$: C 62.43, H 5.73, N 4.55; found: C 62.51, H 5.58, N 4.50.

Log *K* determination: The complexation experiments of pyridine–dendrimer systems were carried out in chloroform that was passed through an alumina column to remove the ethanol (see Figure 2). Dendrimer solutions (6.00×10^{-5} M, 2 mL) containing 0–330 equivalents of pyridine guest were prepared and their electronic spectra were recorded in a 1 cm cuvette. Under the conditions used, zinc–porphyrin dendrimer derivatives gave linear relationship between concentration and Soret band intensity, indicating that they did not self-aggregate. The absorbance values at the Q-band (550 nm) were plotted against the molar ratio of [pyridine ligand]/[dendrimer]. The stability constants were calculated by using nonlinear curve fitting assuming 1:1 complexation. Two or more experiments were done for each combination and the averaged values are listed in Table 1. Such zinc coordination also induced characteristic spectral changes in the Soret region, but the porphyrins had too intense Soret bands to be used in calculation of K values of 10^3 order.

The complexation between thymine and dendrimer was carried out in $CDCl_3$ and monitored by ^{1}H NMR spectroscopy (see Figure 3). The shifted values of amide proton signals were plotted against the molar ratio of [thymine]/[dendrimer], and nonlinear curve fitting assuming 1:1 complexation was applied in the calculation of stability constants.

Determination of the spin–spin relaxation time (T_2): The ^{1}H spin–spin relaxation time (T_2) measurements were performed on a JEOL LA-300 spectrometer at a frequency of 300 MHz using the spin-echo method (CPMG method) contained within the software package. The solvent ($CDCl_3$) was passed through a short alumina column to remove acids just before preparing the samples. Concentration of dendrimer was $2–3\times10^{-3}$ M, and the temperature was maintained at 25°C. The T_2 value was obtained by weighted linear least-square fitting of 11 data points. Two independent experiments were carried out for each sample to evaluate the errors. The T_1 values were also recorded under the same conditions, but their fluctuations were relatively small.

Acknowledgements

The authors are grateful to Dr. D. Paul for his valuable comments on dendrimer synthesis, and also to Professor J. L. Beauchamp of the California Institute of Technology for his kind support on ESI-MS characterization of dendrimer complexes.

[1] a) F. Hof, S. L. Craig, C. Nuckolls, J. Rebek, Jr., *Angew. Chem.* **2002**, *114*, 1556–1578; *Angew. Chem. Int. Ed.* **2002**, *41*, 1488–1508; b) D. Fiedler, D. H. Leung, R. G. Bergman, K. N. Raymond, *Acc. Chem. Res.* **2005**, *38*, 349–358; c) M. Yoshizawa, M. Fujita, *Pure Appl. Chem.* **2005**, *77*, 1107–1112.

[2] Dendrimer receptors of metalloporphyrin type: a) S. Hecht, J. M. Fréchet, *Angew. Chem.* **2001**, *113*, 76–94; *Angew. Chem. Int. Ed.* **2001**, *40*, 74–91; b) S. C. Zimmerman, M. S. Wendland, N. A. Rakow, I. Zharov, K. S. Suslick, *Nature* **2002**, *418*, 399–403; c) T. Imaoka, H. Horiguchi, K. Yamamoto, *J. Am. Chem. Soc.* **2003**, *125*, 340–341; d) W.-S. Li, D.-L. Jiang, Y. Suna, T. Aida, *J. Am. Chem. Soc.* **2005**, *127*, 7700–7702.

[3] Other types of dendrimer receptors: a) F. Diederich, B. Felber, *Proc. Natl. Acad. Sci. USA* **2002**, *99*, 4778–4781; b) M.-C. Daniel, J. Ruiz, J.-C. Blais, N. Daro, D. Astruc, *Chem. Eur. J.* **2003**, *9*, 4371–4379; c) M. Braun, S. Atalik, D. M. Guldi, H. Lanig, M. Brettreich, S. Burghardt, M. Hatzimarinaki, E. Ravanelli, M. Prato, R. van Eldik, A. Hirsch, *Chem. Eur. J.* **2003**, *9*, 3867–3875; d) M. A. C. Broeren, J. L. J. van Dongen, M. Pittelkow, J. B. Christensen, M. H. P. van Genderen, E. W. Meijer, *Angew. Chem.* **2004**, *116*, 3641–3646; *Angew. Chem. Int. Ed.* **2004**, *43*, 3557–3562; e) H.-F. Chow, J. Zhang, *Chem. Eur. J.* **2005**, *11*, 5817–5831.

[4] a) Y. Tomoyose, D.-L. Jiang, R.-H. Jin, T. Aida, T. Yamashita, K. Horie, E. Yashima, Y. Okamoto, *Macromolecules* **1996**, *29*, 5236–5238; b) P. Bhyrappa, G. Vaijayanthimala, K. S. Suslick, *J. Am. Chem. Soc.* **1999**, *121*, 262–263.

[5] a) V. Percec, C. H. Ahn, G. Ungar, D. J. P. Yeardley, M. Möller, S. S. Sheiko, *Nature* **1998**, *391*, 161–164; b) V. Percec, C. M. Mitchell, W.-D. Cho, S. Uchida, M. Glodde, G. Ungar, X. Zeng, Y. Liu, V. S. K. Balagurusamy, P. A. Heiney, *J. Am. Chem. Soc.* **2004**, *126*, 6078–6094; c) C. Böttcher, B. Schade, C. Ecker, J. P. Rabe, L. Shu, A. D. Schlüter, *Chem. Eur. J.* **2005**, *11*, 2923–2928.

[6] a) W. Ong, M. Gómez-Kaifer, A. E. Kaifer, *Chem. Commun.* **2004**, 1677–1683; b) W. Ong, J. Grindstaff, D. Sobransingh, R. Toba, J. M. Quintela, C. Peinador, A. E. Kaifer, *J. Am. Chem. Soc.* **2005**, *127*, 3353–3361.

[7] D. Paul, H. Miyake, S. Shinoda, H. Tsukube, *Chem. Eur. J.* **2006**, *12*, 1328–1338.

[8] a) R. van Heerbeek, P. C. J. Kamer, P. W. N. M. van Leeuwen, J. N. H. Reek, *Chem. Rev.* **2002**, *102*, 3717–3756; b) M. Ooe, M. Murata, T. Mizugaki, K. Ebitani, K. Kaneda, *J. Am. Chem. Soc.* **2004**, *126*, 1604–1605; c) L. S. Kaanumalle, R. Ramesh, V. S. N. M. Maddipatla, J. Nithyanandhan, N. Jayaraman, V. Ramamurthy, *J. Org. Chem.* **2005**, *70*, 5062–5069; d) J. C. Garcia-Martinez, R. Lezutekong, R. M. Crooks, *J. Am. Chem. Soc.* **2005**, *127*, 5097–5103.

[9] a) M.-J. Brienne, J. Gabard, J.-M. Lehn, I. Stibor, *J. Chem. Soc. Chem. Commun.* **1989**, 1868–1870; b) H. Fang, S. Wang, S. Xiao, J. Yang, Y. Li, Z. Shi, H. Li, H. Liu, S. Xiao, D. Zhu, *Chem. Mater.* **2003**, *15*, 1593–1597.

[10] J. S. Lindsey, S. Prathapan, T. E. Johnson, R. W. Wagner, *Tetrahedron* **1994**, *50*, 8941–8968.

[11] B. Forier, W. Dehaen, *Tetrahedron* **1999**, *55*, 9881–9898.

[12] Molecular modeling experiments using MM3 parameters were carried out with CAChe (version 3.2, Fujitsu Ltd., Japan).

[13] Unfortunately, only signal due to dendrimer **6b** was observed in ESI-MS spectrum.

[14] P. Bayon, P. de March, M. Espinosa, M. Figueredo, J. Font, *Tetrahedron: Asymmetry* **2000**, *11*, 1757–1765.

[15] H. Nishiyama, M. Kondo, T. Nakamura, K. Itoh, *Organometallics* **1991**, *10*, 500–508.

Received: January 18, 2006
Revised: June 3, 2006
Published online: October 6, 2006

